



STUDY ON SIMPLE SEMI-ACTIVE CONTROL FOR BASE-ISOLATED STRUCTURE WITH MR DAMPER

Norio IWATA¹ and Satsuya SODA²

SUMMARY

The first part of this paper describes the development of a new type of MR damper. This damper has two by-pass flow portions, which make it possible to independently control the magnetic field in each by-pass in accordance with the direction of the piston rod velocity. The exactness of the damper's generating forces under a simple semi-active control method is examined by excitation and loading tests.

The next part deals with a design formulation for the developed MR damper using a Casson fluid model. It is shown that the formulas predict the relation between the damping force and the piston velocity exactly.

INTRODUCTION

Semi-active control strategies have recently attracted significant attention from many researchers (for example, Niwa[1], Jansen[2], Soda[3], Hidaka[4], Gavin[5], Ribakov[6], Fukukita[7], Dyke[8], Johnson[9][10], Yosida[11], Sahasrabudhe[12], and Yoshioka[13]). These strategies aim to minimize a structure's response by changing the damper's capacity according to the structure's state and the external loads. Of the several kinds of semi-active control devices that have been developed, the Magneto-Rheological fluid (MR) damper seems the most promising, since it has large enough capacity to be applied to large scale buildings and it is readily controlled with a small amount of electric power (for example, Yoshioka[13], Spencer[14][15], Sunakoda[16], Soda[17], Sodeyama[18], Fujitani[19], and Iwata[20]).

Various kinds of semi-active control algorithms have been proposed and extensively studied in various areas. The authors have also proposed a simple semi-active control algorithm for base-isolated structures using an MR damper (Iwata[20][21]). With this method, the MR damper's hysteresis shape is appropriately controlled in order to reduce the isolator's displacement without increasing the acceleration response of the upper structures. We can thus determine the control effectiveness in reducing the system's displacement by measuring the energy dissipation of the MR damper based on the hysteresis shape.

In applying semi-active control including the proposed method to real structures, it is often requested that the damper's force be instantaneously adjustable to the ordered level. However, it is difficult to achieve rapid rise and fall of the force because the magnetic field requires some response time to increase to the ordered level. Therefore, several devices are required to achieve efficient control with MR dampers.

¹ Assist. Prof., Dept. of Architecture, Kinki Univ., Osaka, Japan. Email:iwata@arch.kindai.ac.jp

² Prof., Dept. of Architecture, Waseda Univ., Tokyo, Japan. Email:soda@waseda.jp

This paper first describes a new type of MR damper that has two by-pass flow portions. It was developed to carry out the proposed control exactly, and has two by-passes to make it possible to independently control the magnetic field in accordance with the direction of the piston rod velocity. Two diodes are installed to control the magnetic field in both orifices by using only one power source. The effects of the modified damper are verified by sinusoidal wave excitations and seismic loadings.

The next part deals with the design formulation of the MR damper using a Casson fluid model. Some types of non-Newtonian fluid models have been used to establish the design formulation of the MR damper. This paper studies the exact relation between the velocity and force of the MR damper using the Casson fluid model based on detailed fluid dynamics. In the formulation, the force generation mechanisms are divided into several parts depending on the orifice shape and the fluid's properties. Through this study, the feasibility of MR dampers applied to the structural control will be clarified.

SIMPLE SEMI-ACTIVE CONTROL ALGORITHM

Outline

The author has proposed a simple semi-active control algorithm for base-isolated structures using MR dampers (Iwata[20][21]). In the method, the MR damper's hysteresis shape is controlled as shown in Fig.1.

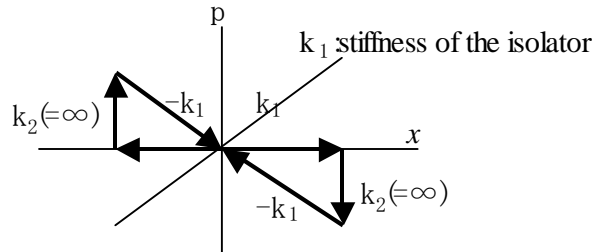


Fig. 1 Hysteresis of the MR damper under the proposed semi-active control algorithm

This algorithm is also represented by:

$$\begin{cases} f_{mr} = -P(x) & x \cdot \dot{x} < 0 \\ f_{mr} = 0 & x \cdot \dot{x} \geq 0 \end{cases} \quad (1)$$

where, x is the isolator's displacement, \dot{x} is the isolator's velocity, f_{mr} is the control force, and $p(x)$ is the isolator's restoring force .

Properties and effectiveness

Response magnification factor

The effectiveness of the proposed control method was verified in a series of analytical and experimental studies (Iwata[20][21]). Response magnification factors were investigated by sinusoidal wave excitation tests using the base-isolated rigid structural model shown in Fig. 2 and 3 (Iwata[20]).

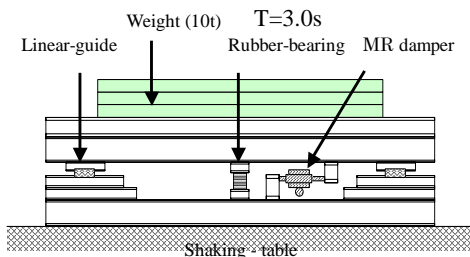


Fig. 2 Rigid base-isolated structural model



Fig.3 Picture of the Rigid base-isolated structural model

Fig. 4 shows the response magnification factors obtained from the sinusoidal excitation tests. In these figures, 0A shows the uncontrolled case, and 0.2A shows the results when a constant current (0.2A) was applied to the damper. Comparing these results, it is found that applying a constant current is effective in reducing the displacement over a wide range of frequencies. However, it is also found that the acceleration response increases in the frequency region higher than about $1.4 p/\omega$, in a similar manner to viscous damping. In contrast, the semi-active control attains a reduction in both displacement and acceleration over a wide range of frequencies.

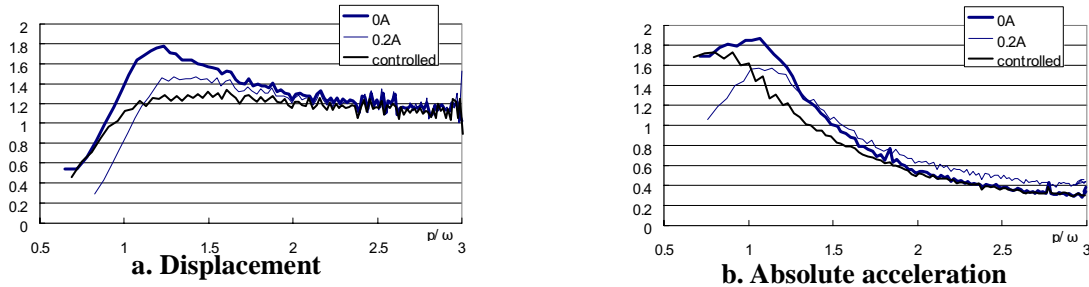


Fig. 4 Response magnification factors obtained by shaking table tests

Seismic wave excitation

The effectiveness under earthquake loads was also clarified by seismic wave excitation tests using the three-story base-isolated structural model shown in Fig.5 (Iwata[21])



Fig. 5 Three-story base-isolated structural model

Fig. 6 shows the peak values and RMS values of the isolator's displacement and the roof floor's absolute acceleration for the test specimens subjected to the El Centro (1940) NS component (maximum ground velocity=50cm/s). When applying a constant current (0.4A), the accelerations rise while the displacements can be effectively reduced. However, the semi-active control reduces the displacement to the same level as with passive control (0.4A) without much increase in acceleration responses. It is thus confirmed that the control method is useful despite its simplicity.

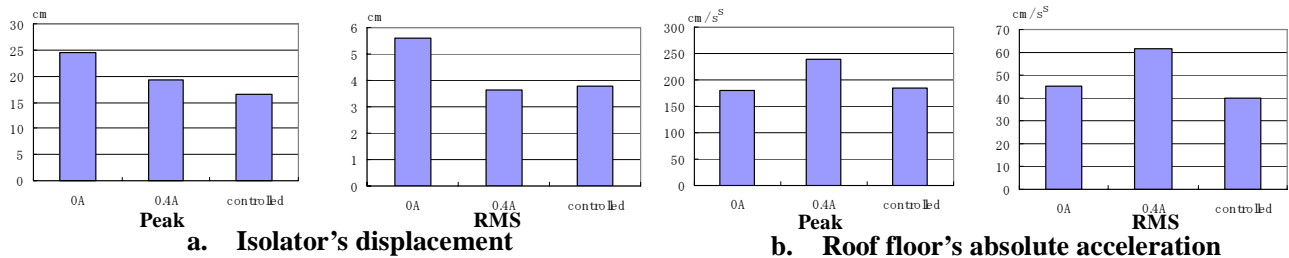


Fig. 6. Response of test specimen (El Centro NS)

Fig. 7 shows the displacement-force relations of the MR damper subjected to two seismic loads. It is confirmed that the MR damper almost reproduced the ideal hysteresis shown in Fig. 1.

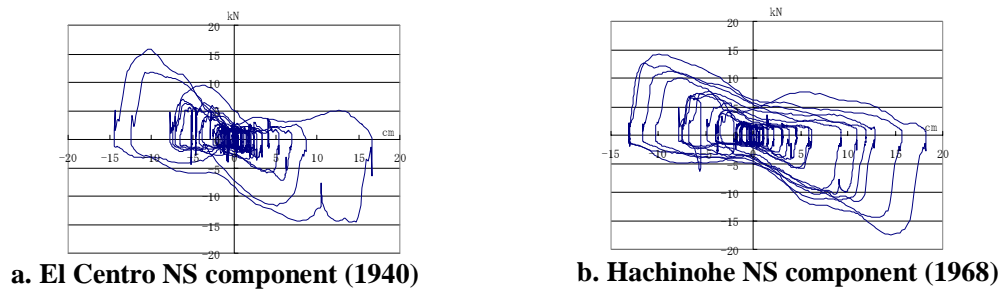


Fig.7 Force-displacement relations of the MR damper subjected to seismic loads

MODIFICATION OF MR DAMPER

In various semi-active control techniques, it is desirable that the damper's force be adjustable instantaneously according changes of the control signals. However, this is not easy because the force requires some response time to rise up/down to the ordered level, especially in rapid stepping-up/down change of the control signals.

As shown in Fig. 7, the hysteresis of the proposed control method can be almost reproduced by a normal (single by-pass) MR damper. However, in detail, a rapid change in the force, corresponding to "k2" shown in Fig. 1, is not adequately reproduced. This insufficiency of the control force may cause deterioration of the control effectiveness.

To overcome this problem, a new type of MR damper, shown in Fig. 8, was developed.

Fig. 9 shows the damper's hydraulic circuit. The damper has a nominal capacity of 20kN, and the basic structure is the same as the already developed 20kN MR damper (Sunakoda[16]). The damper has two by-pass flow portions on each side of the cylinder, which connect two pressure chambers. At the inlets to both by-pass flow portions, two check valves are set up. Each valve allows the fluid to flow in only one direction, which is opposite to that of the other. Therefore, the flow occurs in only one by-pass according to the velocity direction of the piston rod, as shown in Fig. 10. In the middle of each by-pass portion, a rectangular orifice cross-section is installed. Two electromagnets are located on each orifice and are used to generate the variable magnetic field. Using this magnetizing system, independent control of the magnetic field can be carried out in each by-pass. Tab.1 shows the design specification.



Fig. 8 Double by-pass MR damper

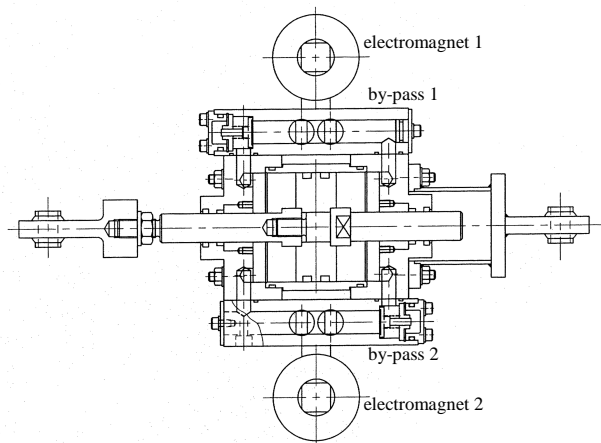


Fig. 9 Hydraulic circuit of the damper

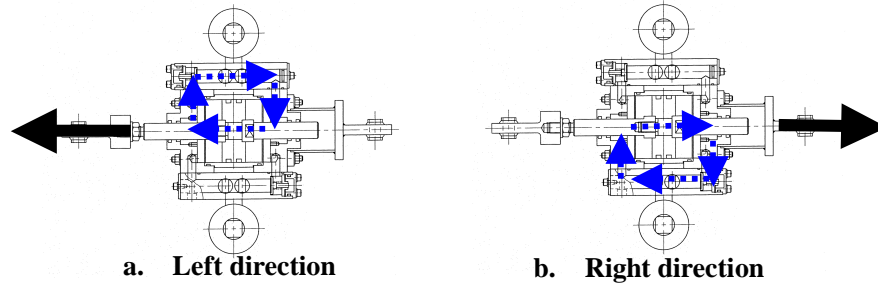


Fig. 10 MR fluid's flow in accordance with the piston velocity direction

Tab. 1 Design specification of the MR damper

Max. force (nominal)	20kN
Stroke	$\pm 35mm$
Cylinder bore	95mm
Orifice size	2mm \times 20mm
Orifice length	20mm
MR fluid	MRF-132LD (LOAD Corp.)
Coil	ϕ 0.5mm 3800turns
Inductance	1.5 henries
Coil resistance	60 ohms
Max. current	0.3A
Manufactured by SANWA TEKKI CORP. (Japan)	

Through sinusoidal and triangle wave excitation tests, the relation between the applied current and the adjustable force was obtained. It was confirmed that this relation was quite similar to the one obtained by the single by-pass damper, which is expressed by the following equation.

$$I[\text{Ampea}] = 0.0025f^2 + 0.091f + 0.0048 \quad (2)$$

In this study, this relation is used to adjust the control force of the MR damper.

Two power sources are required to independently control the magnetic field in both by-pass portions. This makes the system complicated, and also increase the cost. To avoid this, two diodes were installed between the power source and the coils as shown in Fig. 11. With these diodes, current is supplied to only one coil in accordance with the direction (positive/negative) of the current supplied by the power source. Thus, one power source is required to attain the proposed semi-active control. The direction of the current (positive/negative) is set by a PC to be in the same direction as the piston velocity.

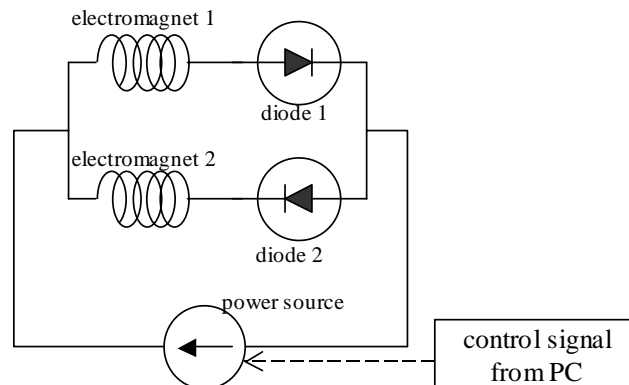


Fig. 11 Electrical circuit with two diodes for current supplying

The amplitude of the current is appropriately decided to become the required force level by the control algorithm and the force-current relation obtained by Eq.(2). As a result, the output current ordered by the PC almost becomes proportional to the piston rod's displacement. Fig. 12 shows the time histories of the current under the proposed control. It was found that the current flowed only in one direction for each electromagnet. The by-pass in which the flow occurs changes at the moment that the piston velocity crosses zero. At that moment, the magnetic field is already formed because the current has already been applied to the orifice before the flow occurs. Therefore, rapid rise and descent of the force are feasible.

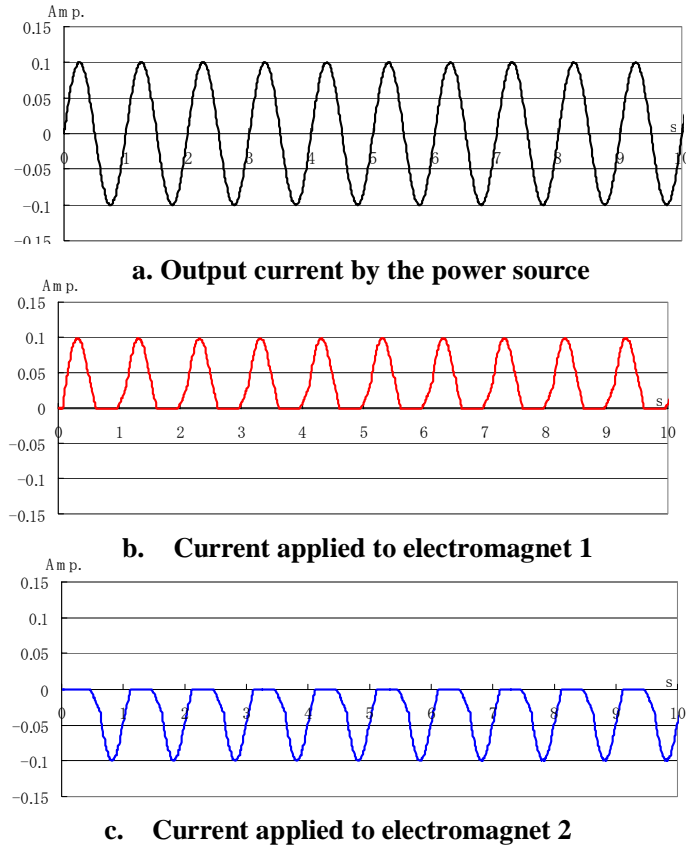


Fig. 12 . Time histories of the applied current under the proposed control by sinusoidal wave (f=1.0Hz, max. current =0.1A)

VERIFICATION OF DAMPER'S PROPERTIES FROM EXCITATION/LOADING TESTS

Triangular wave excitation test

First, we examined the force-displacement relations from triangular wave excitation tests under the proposed control. To verify the effectiveness of the double by-pass system, we compared the hysteresis with that of the single by-pass damper. Assuming application to base-isolated structures, the excitation frequency was set to 0.33Hz. Two gradients in the control hysteresis, shown in Fig. 1 as “k1”, were selected. One was 0.864kN/m and the other 1.73kN/m.

Figs.13 and 14 compare the hystereses of the single by-pass and double by-pass dampers. With the single by-pass damper, rapid rise and fall of the force, which appear at the maximum/minimum values of the piston displacement, can not be perfectly accomplished. This is because the magnetic field can not be formed instantaneously to the rapid change of the electrical current. However, it was found that the double by-pass damper perfectly generates the ideal control force.

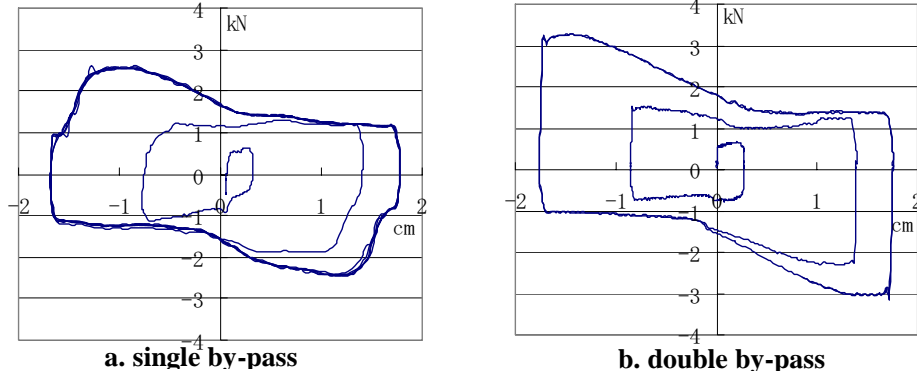


Fig. 13 Comparison of the force-displacement relations
($k_1=0.864\text{kN/m}$, Triangle wave, $f=0.33\text{Hz}$, $\text{Amp.}=1.7\text{cm}$)

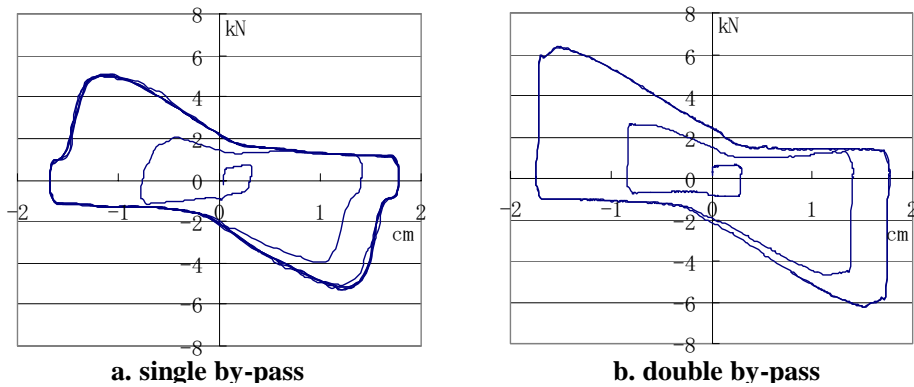


Fig. 14 Comparison of the force-displacement relations
($k_1=1.73\text{ kN/m}$, Triangle wave, $f=0.33\text{Hz}$, $\text{Amp.}=1.7\text{cm}$)

Seismic wave loading tests

Next, seismic wave loading tests were carried out to examine the damper's effectiveness under random loadings. The shaking table and the rigid base-isolated model structures shown in Figs. 2 and 3 were used as the loading system. In this system, the inertia of the model's mass was utilized as the input loads to the damper. The El Centro NS component (1940) and the Hachinohe NS component (1968), whose maximum velocities were set to 15cm/s , were input to the base of the model.

Figs. 15 and 16 compare the hystereses obtained from the test results and the analysis. Good agreement was confirmed between them.

It is clarified that the modified damper can exactly generate the force using the proposed control method.

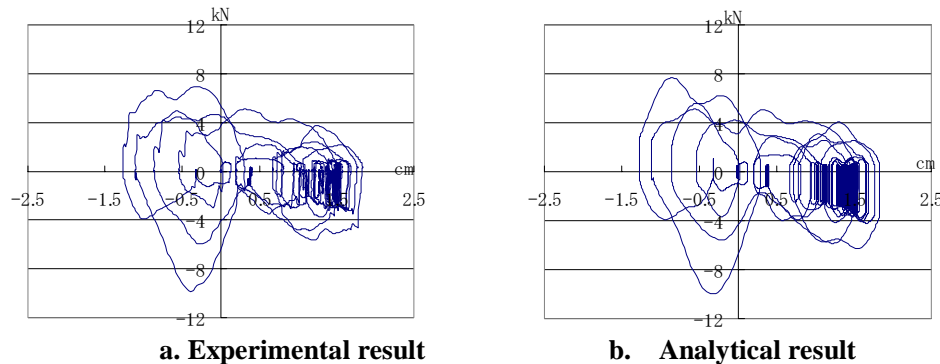


Fig. 15 Comparison of the force-velocity relations for the El Centro NS component (1940)
($k_1=1.768\text{ kN/m}$ Max. 15cm/s)

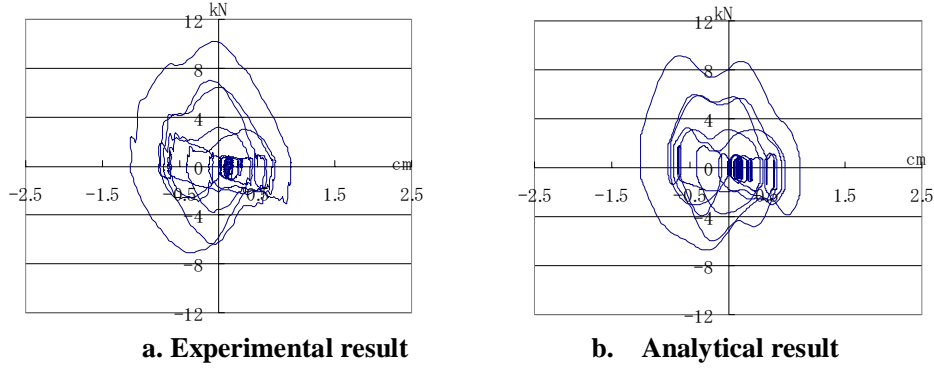


Fig. 16 Comparison of the force-velocity relations for the JMA Kobe NS component (1995) ($k_1=1.768$ kN/m Max. 15cm/s)

DESIGN FORMULATION BY CASSON FLUID MODEL

Basic theory

Some design formulations have been studied using non-Newtonian fluid models to simulate the behaviours of the MR dampers. The Bingham plastic model and the Herschel-Bulkley model have often been used (for example, Sodeyama[22], Wang[23] and Lee[24]).

In the design formulations, we also have to investigate various force generating mechanisms, because the forces are caused by various factors such as the affects of the magnetic field and the orifice shape.

In this study, a design formulation for the developed MR damper is attempted using a Casson fluid model. The basic mechanisms of this damper were exactly the same as those of the ordinary single by-pass MR damper. Therefore, we adopt the method for the single-by-pass MR damper by Sodeyama[22].

Damping force not affected by existence of magnetic fields

Damping force by dynamic pressure at orifice outlet

In this study, the fluid in the by-pass is assumed to be flowing only in the horizontal direction at a speed of u . The generated force caused by this pressure loss is expressed by Eq.(3).

$$F_1 = \frac{1}{2} \rho u_m^2 A_p \quad (3)$$

where ρ is the density of the MR fluid and u_m is the mean velocity of the MR fluid flow at the orifice. A_p is the area on which the fluid pressure in the cylinder acts.

Damping force by friction of seals

The friction force is assumed to be as given by Eq.(4). It is divided to two simple terms (C_1 and C_2). C_1 depends on the pressure inside the damper “ p ”, and C_2 is constant. Each parameter is determined from experimental studies.

$$F_2 = C_1 \cdot \log_e p + C_2 \quad (4)$$

Damping force without magnetic field

Damping force caused by undeveloped laminar flow at inlet

The orifice at the bypass flow section of the MR damper has a rectangular cross-section. The total length of the orifice L is 20mm, which is exposed in the induced magnetic field.

The MR fluid can be assumed to behave as a common Newtonian fluid when not exposed to the magnetic field. The MR fluid enters the orifice at a uniform velocity, as shown in Fig. 17. The flow velocity distribution at each cross-section of the orifice gradually changes due to the viscosity affected by the orifice wall and it finally becomes parabolic.

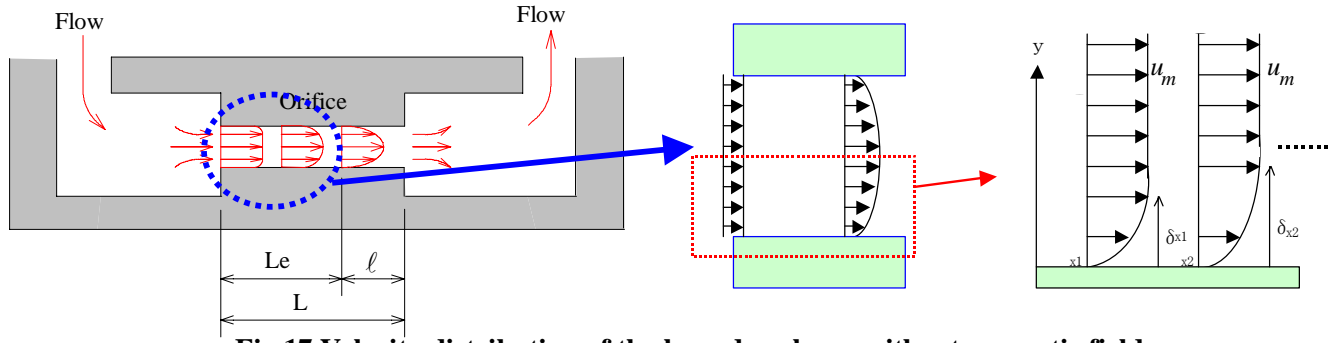


Fig.17 Velocity distribution of the boundary layer without magnetic field

Assuming the integral equation of momentum by Karman, the force generated at the boundary layer laminar flow is expressed by,

$$F_3 = \left(\frac{32}{15}\right)^{\frac{1}{2}} \rho w (u_m^3 \nu L_e)^{\frac{1}{2}} \frac{A_p}{dw} \quad (5)$$

where, ν is the piston velocity, w ($=20mm$) is the width and d ($=2mm$) is the thickness of the orifice. L_e is given by

$$\frac{d^2 u_m}{120\nu} < L : Le = \frac{d^2 u_m}{120\nu}$$

$$\frac{d^2 u_m}{120\nu} \geq L : Le = L$$

Damping force caused by fully developed laminar flow

The force generated by the fully developed laminar flow passing the orifice with a rectangular cross-section is obtained from:

$$F_4 = \frac{12\mu \cdot \ell A_p^2 \nu}{wd^3} \quad (6)$$

where, ℓ is the orifice length with fully developed laminar flow, and μ is the plastic viscosity of the MR fluid.

Damping force caused by magnetic field

The MR fluid flow is assumed to have a plug flow with an identical velocity distribution along the whole orifice length when exposed to the magnetic field as shown in Fig.18.

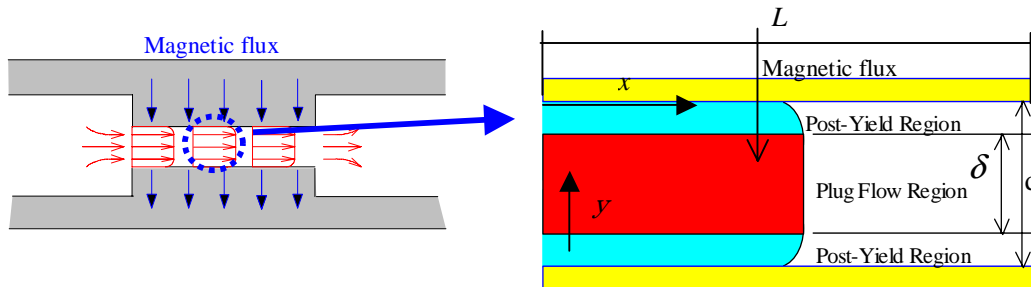


Fig.18 Velocity distribution under magnetic field

In this study, a Casson fluid model was used to simulate the behavior of the MR fluid under the magnetic field. In the Casson model, the relation between the shear strain rate du/dy and the shear stress τ is expressed as

$$\sqrt{\tau} = \sqrt{\tau_0} + \sqrt{\eta_0 \frac{du}{dy}} \quad (7)$$

where, τ_0 is the yield stress of the fluid, and η_0 is a constant depending on the fluids' own mechanical properties.

Considering the orifice shape and the relation between the shear strain rate and the shear stress given by (7), the damping force caused by the magnetic field can be obtained from

$$F_5 = A_p \cdot L \left| \frac{dp}{dx} \right| \quad (8).$$

$\frac{dp}{dx}$ is the pressure gradient, and is given by the volumetric flow rate obtained from

$$Q = A_p \cdot v = w \cdot \frac{1}{2\eta_0} \left| \frac{dp}{dx} \right| \left\{ -\frac{2}{3} y_1^3 + d \cdot y_1^2 + \left(d \cdot \delta + \delta^2 - \frac{4}{3} d \sqrt{d\delta} \right) y_1 + \frac{8}{3} \delta \left(\frac{d}{2} - y_1 \right) \sqrt{\frac{d \cdot \delta}{4} - \frac{\delta \cdot y_1}{2}} - \frac{32}{15} \left(\frac{d}{2} - y_1 \right)^2 \sqrt{\frac{d \cdot \delta}{4} - \frac{\delta \cdot y_1}{2}} - \frac{2}{3} d \cdot \delta \sqrt{d \cdot \delta} + \frac{4}{15} d^2 \sqrt{d \cdot \delta} \right\} \quad (9)$$

where, $y_1 = \frac{d}{2} - \tau_0 \left| \frac{dx}{dp} \right|$ and $\delta = 2\tau_0 \left| \frac{dx}{dp} \right|$.

Total Damping force of MR damper

As discussed above, the damping force of the MR damper can be analyzed on the basis of fluid dynamics. The design formulas for the damping force of the MR damper are summarized as follows.

Damping force without magnetic field:

$$F_w = F_1 + F_2 + F_3 + F_4 \quad (10)$$

Damping force with magnetic field:

$$F_{w0} = F_1 + F_2 + F_5 \quad (11)$$

Verification of design formulation using Casson fluid model

The availability of the above formulation will be confirmed by comparing the analytical results with the experimental ones. Through a series of numerical studies, τ_0 was set to 13000 [Pa] for the applied current of 0.06A, and 18500 [Pa] was set for 0.08A to fit the experimental results. η_0 was set to 0.1[Pa s]. Comparisons between experimental results and analytical ones are shown in Fig. 16. It is found that the analytical and experimental results coincide fairly well for different levels of electric current.

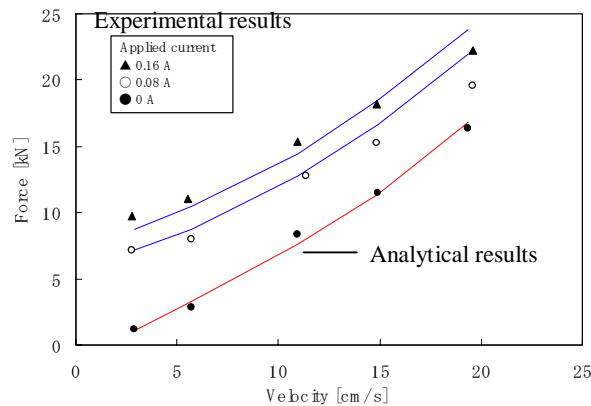


Fig.19 Comparison of the force-velocity relations between analytical and experimental results

CONCLUSIONS

This paper has first experimentally examined the effectiveness of a newly developed double by-pass MR damper. The damper was modified to completely generate the control force using the proposed semi-active control method. We carried out a series of excitation and loading tests to examine the effectiveness of the damper. The experimental results showed that the damper instantaneously generated the control forces when the piston velocity crossed zero. It was clarified that the damper exactly reproduced the hysteresis under the proposed control method.

A design formulation was also attempted using the Casson fluid model. It was found that the adjustable force was exactly predicted by the obtained design formulas consisting of various force generating mechanisms.

ACKNOWLEDGEMENT

This work was partly supported by the 2003 Grants-in-Aid for Young Scientists (B) (No. 15760433) by the Ministry of Education, Culture, Sports, Science and Technology.

The authors would like to acknowledge contributions from the members of the ER/MR working group in the effectors technology section on the Japan side of the US-Japan cooperative research project, "Smart Materials and Structural Systems" (1998-2002).

The shaking tables used in this study belonged to A) the Building Research Institute and B) the National Research Institute for Earth Science and Disaster Prevention in Japan. The authors also wish to thank the members in the institute for their support.

REFERENCES

1. N. Niwa, T. Kobori, M. Takahashi, Y. Matsunaga, N. Kurata and T. Mizuno, "Application of Semi-active Damper System to an Actual Building", *Proc. of the 2nd World Conference on Structural Control*, pp.815-824, 1998
2. L. M. Jansen and S. J. Dyke, "Semiactive Control Strategies for MR Dampers: Comparative Study", *Journal of Engineering Mechanics, ASCE*, 126, pp.795-803, 2000
3. S. Soda and N. Iwata, "Seismic Design of Low to Mid-Rise Building with a Soft First Story Subject to Semi-Active Viscous Damping Control", *12th World Conference on Earthquake Engineering*, No. 1728, 2000
4. S. Hidaka, Y. K. Ahn and S. Morishita, "Structural Control by Damping-Variable Dynamic Damper using ER fluid", *Proc. of the 2nd World Conference on Structural Control*, pp.451-460, 1998
5. H. P. Gavin, R.D. Hanson, "Seismic Protection using ER Damping Walls", *Proc. of the 2nd World Conference on Structural Control*, pp.1183-1190, 1998
6. Y. Ribakov and J. Gluck, "Active Control of MDOF Structures with Supplemental Electrorheological Fluid Dampers", *Earthquake Engineering and Structural Dynamics*, 28, pp.143-156, 1999
7. A. Fukukita, K. Tamura, S. Hayashi and K. Shiba, "Semi-active control of rotational variable damper using electro-rheological fluid", *Journal of Structural Engineering*, Vol. 41B, 1995 (in Japanese)
8. S. J. Dyke, B. F. Spencer Jr., M. K. Sain and J. D. Carlson, "An experimental study of MR dampers for seismic protection", *Smart Materials and Structures*, 7, pp.693-703, 1998
9. E. A. Johnson, G. A. Baker, B. F. Spencer Jr. and Y. Fujino, "Semiactive Damping of Stay Cables", *Journal of Engineering Mechanics, ASCE*, 128(7), 2002
10. E. A. Johnson, J. C. Ramallo, B. F. Spencer, Jr. and M. K. Sain, "Intelligent Base Isolation Systems", *Proc. of the 2nd World Conference on Structural Control*, pp.367-376, 1998
11. K. Yoshida, S. Yoshida and Y. Takeda, "Semi-Active Control of Base Isolation Using Feedforward Information of Disturbance", *Proc. of the 2nd World Conference on Structural Control*, pp.377-386, 1998

12. S. Sahasrabudhe and S. Nagarajaiah, "Sliding Isolated Structures with Smart Dampers", *International Conference on Advances in Structural Dynamics*, pp.335-340, 2000.12
13. H. Yoshioka and B. F. Spencer Jr., "Shaking Table Tests on Semi-active Base Isolation System Employing Magnetorheological Damper", *Proc., Damping Symposium II, JSME*, pp.120-124, 2002 (in Japanese)
14. B. F. Spencer, Jr., G. Yang, J. D. Carlson and M. K. Sain, "Smart Dampers for Seismic Protection of Structures:A Full-Scale Study", *Proc. of the 2nd World Conference on Structural Control*, pp.417-426, 1998
15. B.F. Spencer Jr., S.J. Dyke, M.K. Sain and J.D. Carlson, "Phenomenological Model of a Magnetorheological Damper", *Journal of Engineering Mechanics, ASCE*, 122.pp.179-186, 1997
16. K. Sunakoda, H. Sodeyama, N. Iwata, H. Fujitani and S. Soda, "Dynamic Characteristics of Magneto-Rheological Fluid Damper", *Proc., SPIE's 7th Annual Int. Symposium on Smart Structures and Materials*, No.3989-20, 2000
17. S. Soda, N. Iwata, K. Sunakoda, H. Sodeyama and H. Fujitani, "Experimental and Analytical Methods for Predicting Mechanical Properties of MRF Dampers", *Proc., SPIE's 8th Annual Int. Symposium on Smart Structures and Materials*, No.4330-24,2001
18. H. Sodeyama, K. Sunakoda, H. Fujitani, S. Soda and N. Iwata, "Development of A Magneto-rheological fluid damper for Semi-active Vibration Control Systems of Real Building Structure", *Pro., 15th International Conference on MOTION and VIBRATION CONTROL*, pp.725-730,2000
19. H.Fujitani, H. Sodeyama, K. Hata, N. Iwata, Y. Komatsu, K. Sunakoda and S. Soda, "Dynamic Performance Evaluation of Magneto-Rheological Damper", *International Conference on Advances in Structural Dynamics*, pp.319-326, 2000
20. N. Iwata, K. Hata, H. Sodeyama, K. Sunakoda, H. Fujitani, T. Hiwatashi, Y. Shiozaki and S. Soda, "Application of MR damper to base-isolated structures", *Proc., SPIE's 9th Annual Int. Symposium on Smart Structures and Materials*, No.4696-45, 2002
21. N. Iwata, H. Sodeyama, K. Sunakoda, K. Hata, T. Hiwatashi, Y. Shiozaki, H. Fujitani, and S. Soda, "Experimental Study on the Effectiveness of a Simple Semi-Active Control Algorithm for Base-Isolated Structures", *The 11th Japan Earthquake Engineering Symposium*, No.326, pp. 1761-1766, 2002
22. H. Sodeyama, N. Iwata, and K. Sunakoda, "Sturdy on the Force-Velocity Relationship of By-Pass Type MR Damper", *Journal of Structural Engineering*, Vol. 48B, pp.517-523, 2002 (in Japanese)
23. X. Wang and F. Gordaninejad, "Study on field-controllable, electro- and magneto- rheological fluid dampers in flow mode using Herschel-Bulkley theory", *Proc., SPIE's 7th Annual Int. Symposium on Smart Structures and Materials*, 232-243, 2000
24. D. Y. Lee and N. M. Wereley, "Analysis of electro- and magneto- rheological flow mode dampers using Herschel-Bulkley model", *Proc., SPIE's 7th Annual Int. Symposium on Smart Structures and Materials*, 244-255, 2000